Optimization of calmodulin-affinity chromatography for brain and organelles

Kulej, Katarzyna ; Sidoli, Simone; Palmisano, Giuseppe; Edwards, Alistair; Robinson, P. J.; Larsen, Martin Røssel

Published in:
EuPA Open Proteonomics

DOI:
10.1016/j.euprot.2015.05.004

Publication date:
2015

Document version
Final published version

EuPA Open Proteomics 8 (2015) 55–67

Contents lists available at ScienceDirect

EuPA Open Proteomics

journal homepage: www.elsevier.com/locate/euprot

Optimization of calmodulin-affinity chromatography for brain and organelles

Katarzyna Kulej[a], Simone Sidoli[a], Giuseppe Palmisano[a], Alistair V.G. Edwards[a], Phillip J. Robinson[b], Martin R. Larsen[a,*]

[a] Department of Biochemistry and Molecular Biology, University of Southern Denmark, Campusvej 55, DK-5230 Odense, Denmark
[b] Cell Signalling Unit, Children's Medical Research Institute, The University of Sydney, Westmead, Australia

ARTICLE INFO

Article history:
Received 15 March 2015
Received in revised form 16 May 2015
Accepted 22 May 2015
Available online 23 July 2015

Keywords:
Calmodulin
Calmodulin-binding proteins
Affinity purification
Mass spectrometry
Phosphorylation

ABSTRACT

Calmodulin (CaM) is a Ca^{2+}-binding signaling protein that binds to and activates many target proteins, known as calmodulin-binding proteins (CaM-BPs). They are involved in multiple cellular processes. Despite the diversity and importance of CaM-BPs, many remain to be identified and characterized. We performed extensive optimization of a CaM-affinity capture method, using commercial CaM-chromatographic material. We identify both the Ca^{2+}-dependent and -independent CaM binding proteomes in both mouse brain and in rat brain neuronal organelles, synaptosomes, and compared cytosolic with membrane associated targets. Fractionation of peptides, derived from on-resin tryptic digestion, using hydrophilic interaction liquid chromatography (HILIC) was combined with reversed-phase liquid chromatography tandem mass spectrometry (LC-MS/MS) to improve identification of low abundance CaM-BPs in a reproducible and sensitive manner. Various detergents were tested for the most efficient membrane protein solubilization for pull-down of membrane-associated CaM-BPs. We identified 3529 putative mouse brain CaM-BPs, of which 1629 were integral membrane or membrane-associated. Among them, 170 proteins were known CaM-BPs or previously reported as potential CaM-BPs while 696 contained predicted CaM binding motifs. In synaptosomes we identified 2698 CaM-BPs and 2783 unique phosphopeptides derived from 984 of the potential synaptosomal CaM-BPs. Overall, our improved workflow provides unmatched sensitivity for the identification of the CaM binding proteome and its associated phosphoproteome and this now enables sensitive analysis of organelle-specific CaM-BPs.

1. Introduction

Calmodulin (CaM) is the first and best studied example of the EF-hand family of Ca^{2+}-sensing proteins. It is one of the most conserved eukaryotic proteins known [1,2]. CaM constitutes at least 0.1% of the total cellular protein concentration in many cells and it is expressed at higher levels in the brain, testis, excitable cells and rapidly growing cells. It participates in signaling pathways that regulate processes such as cell proliferation, learning and memory, growth, exocytosis, endocytosis and movement [3]. Regulation of these events is exerted via direct interactions of CaM with a large number of proteins, including kinases, phosphatases, and cytoskeleton proteins, in response to a rise in intracellular Ca^{2+} concentration. In addition, in the nucleus CaM transmits Ca^{2+} signals to a number of transcription factors [4–6].

CaM is predominantly a helical protein composed of the N- and C-terminal globular domains connected by a central flexible helix. Each globular domain contains two Ca^{2+}-binding sites of the helix-loop-helix (EF-hand) type [7]. The biological action of CaM is defined by its biophysical properties, including cooperative Ca^{2+} binding [8] and structural autonomy of two globular domains [9] which cooperate in target binding [10–13]. Binding of Ca^{2+} to CaM causes a conformational change that exposes several hydrophobic patches on the CaM surface, producing an "*open*" CaM conformation, which allows CaM to bind amphipathic α-helices in target proteins. CaM can also bind proteins in the non-Ca^{2+} form (the *apo* isoform) or partially Ca^{2+} saturated forms (two Ca^{2+} ions bound to the C-terminal domain).

Calmodulin binding proteins (CaM-BPs) are a large and diverse group of proteins, solely related by the fact that they interact with CaM. Based upon their Ca^{2+} requirement for CaM binding, they can

* Corresponding author.
E-mail address: mrl@bmb.sdu.dk (M.R. Larsen).

http://dx.doi.org/10.1016/j.euprot.2015.05.004

be classified into two categories of interaction: Ca^{2+}-dependent and Ca^{2+}-independent. Members of the two categories have several poorly defined amino acid sequence motifs for CaM binding. Among many Ca^{2+}-dependent CaM-BPs there may be one or more CaM binding domains of approximately 20 amino acid residues in length, which have the capacity to form amphipathic α-helices with both basic and hydrophobic faces of CaM [2,14]. Motif identification is mostly performed by comparative studies of the many reported CaM binding regions from different proteins. However, CaM binding motif analyses for these regions provide many false positives due to the relaxed consensus motifs. Ca^{2+}-dependent CaM-BPs have been grouped according to two related motifs they may contain, called 1-8-14 and 1-5-10, based on the position of conserved hydrophobic residues [15,16]. Proteins containing the 1-8-14 motif include nitric oxide synthase, adenylyl cyclase and skeletal muscle myosin light chain kinase [16,17], whereas CaM dependent kinases (CaMKI, II) and synapsin, contain the 1-5-10 motif [18]. Many Ca^{2+}-independent CaM-BPs contain an IQ motif consensus sequence, such as the one found in conventional type II myosin light chains, unconventional myosins, neuromodulin and neurogranin [19]. However, the Ca^{2+} sensitivity of proteins containing IQ motif appears to be highly variable and some of them can bind to CaM or other EF-hand proteins in a Ca^{2+}-dependent manner [20]. Although these criteria are all useful for classification and sometimes for identification of new CaM binding domains in target proteins, CaM also interacts with amino acid sequences that have no homology to any of these motifs. Similarly, some proteins containing CaM binding motifs may not directly interact with CaM [16]. Binding of CaM can also be regulated by post-translational modifications (PTMs) of CaM-BPs, such as phosphorylation [15].

More specific methods are required to purify and identify potential CaM-BPs to construct the "calmodulin interactome" and increase our understanding of CaM target recognition, since comparative and predictive analyses are largely insufficient to identify new potential CaM-BPs, Affinity purification-mass spectrometry (AP-MS), coupled to advances in the field of bioinformatics, has previously been used to identify hundreds of CaM-BPs [21–24]. Therefore our aim was to optimize a protocol for the selective enrichment of CaM-BPs using commercial CaM-affinity chromatography material with sufficient sensitivity to apply the method to identify CaM-BPs from subcellular organelles as well as to identify PTMs on CaM-BPs, e.g. phosphorylation, which requires more starting material. Our optimized strategy allowed greatly improved detection of CaM-BPs in whole brains and to identify both the synaptosome CaM interactome as well as the phosphoproteome of this organelle for the first time.

2. Materials and methods

2.1. Materials

All chemicals were purchased from Sigma–Aldrich (St Louis, MO, USA), unless otherwise stated. Titanium dioxide (TiO_2) was a gift from GL Sciences (Tokyo, Japan). Sequence-grade trypsin was from Promega (Madison, WI, USA). Benzonase was obtained from MERCK (Merck & Co., Inc., NJ, USA). Lysyl endopeptidase (Lys-C), mass spectrometry grade was from Wako (Richmond, VA, USA). Complete EDTA-free protease inhibitor and phosphatase inhibitor cocktail tablets were from Roche Applied Science (Mevlan, France). Poros Oligo R3 reverse phase chromatographic material was from PerSeptive Biosystems (Framingham, MA, USA). Reprosil-C18 3 μm beads were from MikroLab Aarhus S/A (Højbjerg, Denmark). 3 M Empore™ C8 and C18 disks were from 3 M Bioanalytical Technologies (St. Paul, MN, USA). TSKgel Amide-80HILIC (3 μm particles) was from Tosoh Bioscience (Stuttgart, Germany). 2.5 ml empty columns (bottom plug 35 nm pore size) were from Thermo Fisher Scientific. Crude CNBr-activated Sepharose™ 4B resin was from GE Healthcare Life Sciences (GE Healthcare Europe GmbH, Denmark). Calmodulin Sepharose™ 4B was from Stratagene (Agilent Technologies, USA). Microcon filtration devices were from Millipore (Millipore, Bedford, MA, USA). NuPAGE 1DE System was from Invitrogen (Invitrogen, Life Technologies™; USA). All other reagents used in the experiments were of at least sequencing grade. All solutions were made with ultrapure Milli-Q water (Millipore, Bedford, MA, USA).

2.2. Biological material – mouse brain tissue and synaptosomes

Postnatal 21 days old mice (C57BL/6, males) were euthanized by decapitation and total brain matter removed, immediately snap-frozen in liquid nitrogen and stored at −80 °C. Animal experiments were performed according to the ethics guidelines of the Society of Laboratory Animal Science. Frozen tissue (~0.5 g) was homogenized in liquid nitrogen following with homogenization of brain powder in 3.5 ml lysis buffer containing 50 mM tris-HCl, 150 mM NaCl, 1 mM DTT, 4 mM EGTA, benzonase, 0.1 mM sodium pervanadate, protease inhibitor cocktail, phosphatase inhibitor cocktail, pH 7.5, by Dounce homogenization and probe tip sonication at 4 °C. The lysate was shaken at 4 °C for 1 hour and ultracentrifuged at 100,000×*g* for 1.5 h at 4 °C. After centrifugation, the supernatant containing primarily cytosolic proteins was collected. The remaining membrane pellet was dissolved by probe tip sonication in the lysis buffer used above supplemented with 1% detergent (Table 1; lists the detergents used). Subsequently, the membrane homogenate was ultracentrifuged according to the conditions described above. After ultracentrifugation, the supernatant enriched in the membrane proteins was collected. Synaptosomes were purified accordingly to the Percoll method of Dunkley et al., [25]. For the purpose of this study, F4 and F3 fractions from the Percoll gradient were pooled together. Protein concentrations were determined by amino acid analysis (AAA) on a Biochrom 30 amino acid analyzer (Biochrom, Cambridge, UK).

2.3. CaM-affinity chromatography

CaM-Sepharose 4B beads as a 50% slurry were transferred to a 2.5 ml volume empty column (bottom plug 35 nm pore size) to the final volume of 0.5 ml (volume of beads is estimated as settled slurry) and equilibrated with 10 bed volumes of equilibrium buffer containing 50 mM tris-HCl, 150 mM NaCl, pH 7.5, in the presence of either 2 mM $CaCl_2$, 1 mM $MgCl_2$ or 4 mM EGTA to study Ca^{2+}-dependent or Ca^{2+}-independent CaM interactions. To not overload the resin capacity (1–2 mg of purified proteins/ml of

Table 1
Detergents used in the study of membrane CaM-BPs. Abbr: *n*-dodecyl-β-D-maltoside (DDM); *n*-octyl-β-D-glucopyranoside (β-OG); FOS-CHOLINE-16 (FC-16); sodium deoxycholate (SDC).

No.	Type of detergent	Name of detergent	Concentration	CMC value [mM] (20–26 °C)
1	Non-ionc	DDM	1%	~1.6
2		β-OG	1%	~23–25
3		Triton X-100	1%	~0.22–0.24
4		Triton X-114	1%	~0.2
5		NP-40	1%	~0.29
6		Digitonin	1%	<0.5
7	Zwittergent	Zwittergent 3-10	1%	~39
8		Zwittergent 3-16	1%	~0.010–0.060
9		FC-16	1%	~0.013
10	Bile salt	SDC	1%	~2–6

settled resin; estimated by the supplier), a 1:1 ratio of sample (mg) to settled resin (ml) was used. The cell cytosol lysate (0.5 mg of total crude proteins) was incubated on the shaker with CaM-Sepharose 4B beads for different times (1 h at room temperature, 2 h at 4 °C or overnight at 4 °C) in the presence of 8 mM $CaCl_2$, 4 mM $MgCl_2$ or 4 mM EGTA accordingly. Subsequently, the beads were washed with 10 bed volumes of a set of equilibrium buffers containing increasing salt-concentrations ([NaCl]) from 150 mM to 5 M NaCl, until A_{280} became undetectable, followed by a last wash step with the equilibrium buffer containing 150 mM NaCl. The last wash step was performed in order to remove the excess of salt remaining on the beads. The 0.1 M tris-HCl buffer pH 8.0 treated CNBr-activated Sepharose 4B resin was used as a background binding control. In experiment including membrane proteins, the equilibrium buffer was supplemented with 0.25% detergent (Table 1).

2.4. Elution of bound proteins

Three methods were tested to elute CaM-BPs from the affinity resin. Method 1 and method 2 were used sequentially, while method 3 was used independently.

Method 1: In the first approach the bead-bound proteins were eluted by 2 h incubation of resin at RT with the Ca^{2+} ion chelator EGTA (50 mM tris-HCl, 150 mM NaCl, 10 mM EGTA, pH 7.5), followed by an additional wash with 6 bed volumes of the same buffer. The columns were centrifuged at 1000×*g* for 5 min to remove any residual elution buffer. Samples were concentrated to ~200 μl by lyophilization, reduced with 10 mM dithiothreitol (DTT) for 45 min at RT and carbamidomethylated with 20 mM iodoacetamide (IAA) for 45 min at RT in the dark. Subsequently, samples were digested with trypsin at an enzyme to substrate ratio of approximately 1:50 for 12 h at 37 °C. The samples were acidified with 100% formic acid (FA) to pH ≤ 3 and the peptides were desalted using Poros Oligo R3 RP micro-columns packed in a P200 stage tip with C18 3 M plug. Purified peptide samples were lyophilized and stored at −20 °C for further analysis.

Method 2: In the second approach, beads after performing *Method 1* were incubated 2 h at RT with 5% SDS, 40% methanol, following with boiling and bead washing with 6 bed volumes of the same buffer. The columns were centrifuged at 1000×*g* for 5 min to remove any residual elution buffer. The SDS detergent was removed from these samples by precipitation using chloroform ($CHCl_3$)-methanol (MeOH) precipitation [26]. The protein pellet from $CHCl_3$–MeOH precipitation was resuspended in 6 M urea and 2 M thiourea. Samples were reduced and alkylated as described above. After alkylation proteins were digested first with endopeptidase Lys-C for 3 h, after which the solution was diluted 10 times with 50 mM triethylammonium bicarbonate buffer (TEAB), and then sonicated on ice. Subsequently, samples were trypsin digested and desalted as described above.

Method 3: In the third approach proteolytic digestion was performed directly on CaM-affinity beads (with no prior elution by *Method 1* or *2*). After the final wash with 150 mM NaCl equilibrium buffer the CaM-affinity column was closed and resin was resuspended with 1 ml of 50 mM TEAB. Proteins were reduced with 10 mM DTT for 1 h at RT followed by alkylation with 20 mM IAA for 1 h at RT in the dark with shaking. The reduced and alkylated samples were digested on the CaM column with trypsin solution at an enzyme to substrate ratio of 1:50 (taking into account additional amount of CaM protein on the resin) in the presence of 20% ACN for 12 h at 37 °C, with continuous rotation. Organic solvent-assisted digestion was used in order to improve efficiency of trypsin digestion as previously was shown [27–32]. The peptides were eluted from the column by centrifugation at RT, 1000×*g* for 5 min. The CaM-affinity beads were then washed with 4 bed volumes of 30% ACN, 50 mM TEAB to remove peptides absorbed by hydrophobic interactions. Both recovered eluates were pooled in low binding eppendorf tubes (Sorenson, BioScience, Inc., West Salt Lake City, Utah, USA) and concentrated to ~200 μl by lyophilization. Trypsin activity was inhibited by acidification with 100% FA to pH ≤ 3. Subsequently, samples were desalted using Poros Oligo R3 RP micro-columns. The purified peptide samples were lyophilized and stored at −20 °C for further analysis.

The final protein concentration in each eluate was determined by AAA. In relation to the on-CaM-resin tryptic digestion, control sample with crude CaM-Sepharose resin was digested with trypsin in order to evaluate the concentration of CaM protein on the resin. The on-CaM-resin tryptic digestion elution was used in the most of the optimized conditions, unless otherwise stated.

2.5. Enrichment of phosphopeptides from rat synaptosomes by TiO_2 chromatography

CaM-affinity chromatography of rat brain synaptosomes was performed using the same approach as for mouse brain tissue. On-CaM-resin tryptic digestion (third approach) was used to elute bead-bound proteins. The eluate was concentrated to 100 μl by lyophilization. Subsequently, the TiO_2 enrichment of phosphopeptides was performed as previously described [33]. The lyophilized phosphorylated peptide samples were reconstituted in 0.1% trifluoroacetic acid (TFA) and desalted using Poros Oligo R3 RP micro-columns. For identification of the synaptosome CaM-BPs, unbound peptides from the TiO_2 (flow-through, FT) and subsequent TiO_2 washes were combined and lyophilized to produce a non-modified peptide fraction. The non-modified peptide fraction was resuspended in 0.1% TFA and desalted using Poros Oligo R3 RP micro-columns. The peptide samples were subsequently lyophilized and stored at −20 °C for further analysis.

2.6. SDS–PAGE and in-gel digestion

For protein separation by SDS–PAGE the NuPAGE 1DE System was used (NuPAGE Novex 4–12% bis–tris 1.0 mm gels, Invitrogen, USA). Visualization of separated proteins was performed by overnight staining with Coomassie blue G-250 solution. The in-gel tryptic digestion followed by peptide extraction from the gel bands was performed accordingly to [34]. The extracted peptides were desalted using Poros Oligo R3 RP micro-columns prior to LC–MS/MS analysis.

2.7. Capillary hydrophilic interaction liquid chromatography (capillary-HILIC)

Capillary-HILIC was performed as previously described [35]. The collected peptide fractions were lyophilized and subsequently resuspended in 0.5% FA prior to analysis by LC–MS/ MS.

2.8. Reversed phase liquid chromatography tandem mass spectrometry (LC–MS/MS)

The peptides were separated by LC equipped with an in-house packed 17 cm × 100 μm Reprosil-Pur C18-AQ column (3 μm; Dr. Maisch GmbH, Germany) using an EASY-LC nano-HPLC (Thermo, Proxeon, Odense, Denmark). The HPLC gradient was 0–34% solvent B (*A* = 0.1% FA; *B* = 95% ACN, 0.1% FA) at a flow rate of 250 nl/min. MS analysis was performed using an LTQ Orbitrap XL or an LTQ Orbitrap Velos (Thermo Scientific, Bremen, Germany). An MS scan (350–2000 *m*/z) was recorded in the Orbitrap at a resolution of 60,000 in the Orbitrap XL and in the Orbitrap Velos, with an automatic gain control of 1e6 ions. For analysis of peptides

obtained from CaM-BPs, data-dependent CID MS/MS analysis was performed on the top 5–7 most intense ions in the Orbitrap XL and top 10 in the Orbitrap Velos. MS/MS parameters were as follows; activation time = 15–30 ms in the Orbitrap XL and 5 ms in the Orbitrap Velos, normalized collision energy = 35, Q-activation = 0.25, dynamic exclusion = enabled with repeat count 1, exclusion duration = 60 s and intensity threshold = 20,000. Phosphopeptides were analyzed using the same acquisition method, but setting the intensity threshold for data-dependent acquisition to 30,000.

2.9. Data analysis

Raw mass spectrometer files were analyzed using Proteome Discoverer (v1.4, Thermo Scientific, Bremen, Germany). MS/MS spectra were converted to mgf files and searched against the UniProt Rodents database using Mascot (v2.3.02, Matrix Science, London, UK). Database searches were performed with the following parameters: precursor mass tolerance 10 ppm; MS/MS mass tolerance 0.6 Da. Trypsin with the possibility of two missing cleavages was selected on the enzyme specification. Cysteine carbamidomethylation was specified as fixed modification. Variable modifications included: methionine oxidation; serine, threonine and tyrosine phosphorylation; asparagine and glutamine deamidation. Results were filtered for 1% false discovery rate calculated using Percolator. Peptides with a Mascot ion score <20 were removed and only rank 1 peptides were accepted. Label-free quantification was performed with either Proteome Discoverer and with Progenesis LC–MS (v4.1, Nonlinear Dynamics, Newcastle upon Tyne, UK). Proteome Discoverer was used for quantification of HILIC or gel fractionations by using the precursor area detector node with an event detector of 2 ppm. Proteins were considered as valid if at least one unique peptide was quantified. Progenesis were adopted to quantify experiments without the presence of fractions using medium settings of feature extraction and automatic chromatography alignment. Gene ontology (GO) annotation was retrieved by UniProt database (http://www.uniprot.org) [36], ProteinCenter (Proxeon, Thermo Fisher Scientific) and the GOrilla software (Gene Ontology enRIchment anaLysis and visuaLizAtion tool) [37,38]. A web-based database (Calmodulin Target Database, http://calcium.uhnres.utoronto.ca/ctdb) was used for identification of putative CaM binding motifs [39]. A number of curated public databases dedicated to protein–protein interactions (PPI), such as IntAct [40], STRING [41], BIND [42], MINT [43], BioGRID [44], DIP [45], HitPredict [46] or HPRD [47], were used to validate primary CaM-BPs. To clarify the total number of identified cytosol and membrane proteins, the protein lists obtained from cytosol and membrane faction was further analyzed for presence of peripheral membrane (PM) and transmembrane (TM) motifs using the ProteinCenter software. Subsequently, proteins containing CaM binding motif and PM/TM domains were classified as true membrane CaM-BPs, and remaining proteins as cytosolic CaM-BPs.

3. Results and discussion

A number of optimization experiments were performed to develop a protocol for CaM-affinity chromatography to identify the CaM interactome and its phosphoproteome from mouse brain tissue and rat synaptosomes, in a high-throughput manner. The process of sample preparation was optimized in order to analyze cytosolic and membrane bound CaM-BPs. Affinity chromatography was performed in the presence of either Ca^{2+} ions or EGTA to distinguish between Ca^{2+}-dependent and -independent interactions. To maximize the number of CaM-BP identifications, experiments were conducted under different conditions designed to optimize various affinity chromatography stages (see Fig. 1 and Fig. S1 for details of experimental workflows). Optimization of CaM affinity chromatography was performed based on CaM-BPs predicted from the Calmodulin Target Database.

Supplementary material related to this article found, in the online version, at http://dx.doi.org/10.1016/j.euprot.2015.05.004.

3.1. Increased CaM-BP availability by EGTA pretreatment

To achieve the highest concentration of free CaM-BPs prior to CaM-affinity chromatography the tissue homogenate was first incubated with EGTA to obtain more CaM-BPs to interact with the CaM immobilized on the resin. The lysate was then mixed with CaM-affinity resin (1:1 ratio of proteins (mg): resin (ml)) with an excess of $CaCl_2$ to block the EGTA and provide free Ca^{2+} ions for binding of CaM-BPs to the affinity resin. The results of the

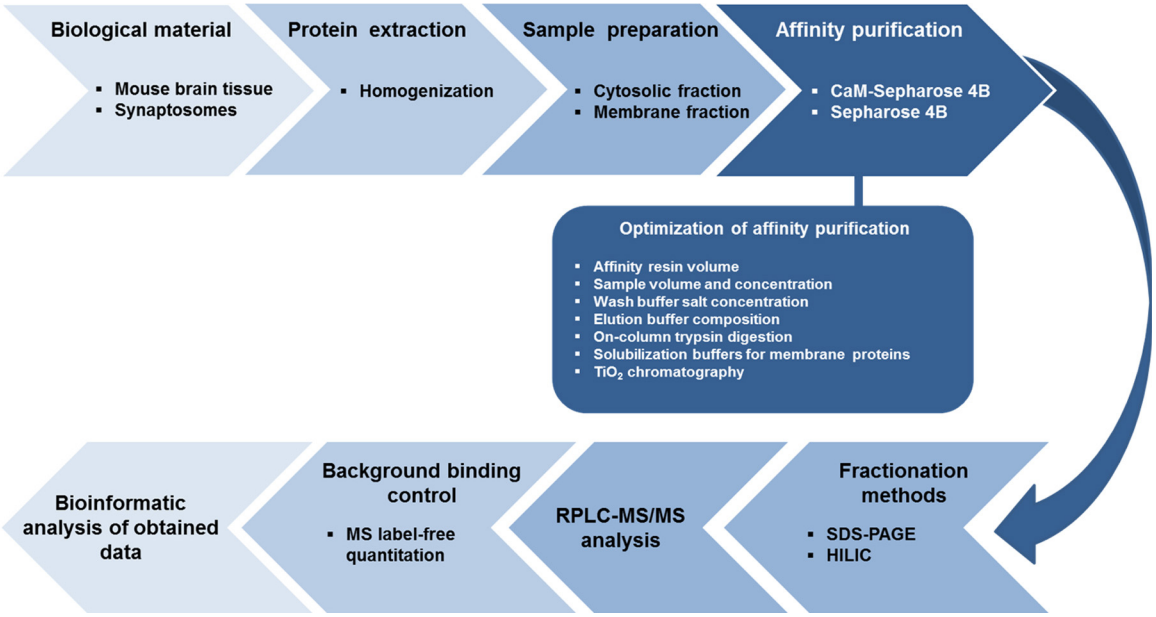

Fig. 1. Experimental workflow. In the figure, all the steps where optimization was performed are displayed. The affinity purification step was the one where most of the improvements were achieved.

pull-down of CaM-BPs with EGTA pre-treated and non-treated samples were compared using LC–MS/MS analysis and label free quantitation. A total of 794 proteins were identified between the two conditions, with no missing values. In both conditions we observed a similar number of potential CaM-BPs. However, EGTA pre-treatment specifically increased the yield of known CaM-BPs in the eluate, including low abundant CaM-BPs. Some of these were Ca^{2+}/CaM-dependent protein kinase type II (subunit α, CaMK2α), calcineurin, neuromodulin (Gap43) and synapsin-1 (Figure S2 and Table S1A). Interestingly, known Ca^{2+}-independent CaM-BPs such as neuromodulin also showed increased abundance after EGTA pre-treatment.

Supplementary material related to this article found, in the online version, at http://dx.doi.org/10.1016/j.euprot.2015.05.004.

3.2. Ratio of tissue lysate to CaM-affinity resin

The effects of volume of sample solution as a function of binding efficiency to the CaM-resin were investigated. We first fixed the amount of resin (0.5 ml) and varied the brain extract volume loaded keeping constant the protein amount (0.5 mg). Total CaM-BP bound was assessed by amino acid composition analysis (AAA). A 1:3 resin: sample volume ratio provided the most efficient binding (>200 μg of proteins) (Fig. 2A). High protein concentrations sometimes lead to protein aggregation, precipitation and column blockage (data not shown). The resin volume was then varied (0.1–0.75 ml) while the protein load was fixed and revealed a linear increase in the amount of affinity purified proteins (Fig. 2B). Despite that 0.25 mg of proteins is sufficient for traditional MS-based quantitative proteomics workflows, PTMs are substoichiometric and require in many cases more starting material.

3.3. Reducing non-specific binding to the CaM-affinity resin

To reduce nonspecific binding to the CaM resin the effect of time of incubation was tested in a quantitative manner. The relative abundance of bound CaM-BP after enrichment as compared to the total protein abundance was not different between 1 h incubation of tissue lysates at RT or 2 h incubation at 4 °C (Fig. S3; Table S1B). However, the loss of CaM interactors and the increase in the association of contaminants was evident after overnight incubation at 4 °C. All subsequent experiments were performed for 2 h at 4 °C to minimize potential loss of labile phosphorylation by any remaining active endogenous phosphatases. Furthermore, the

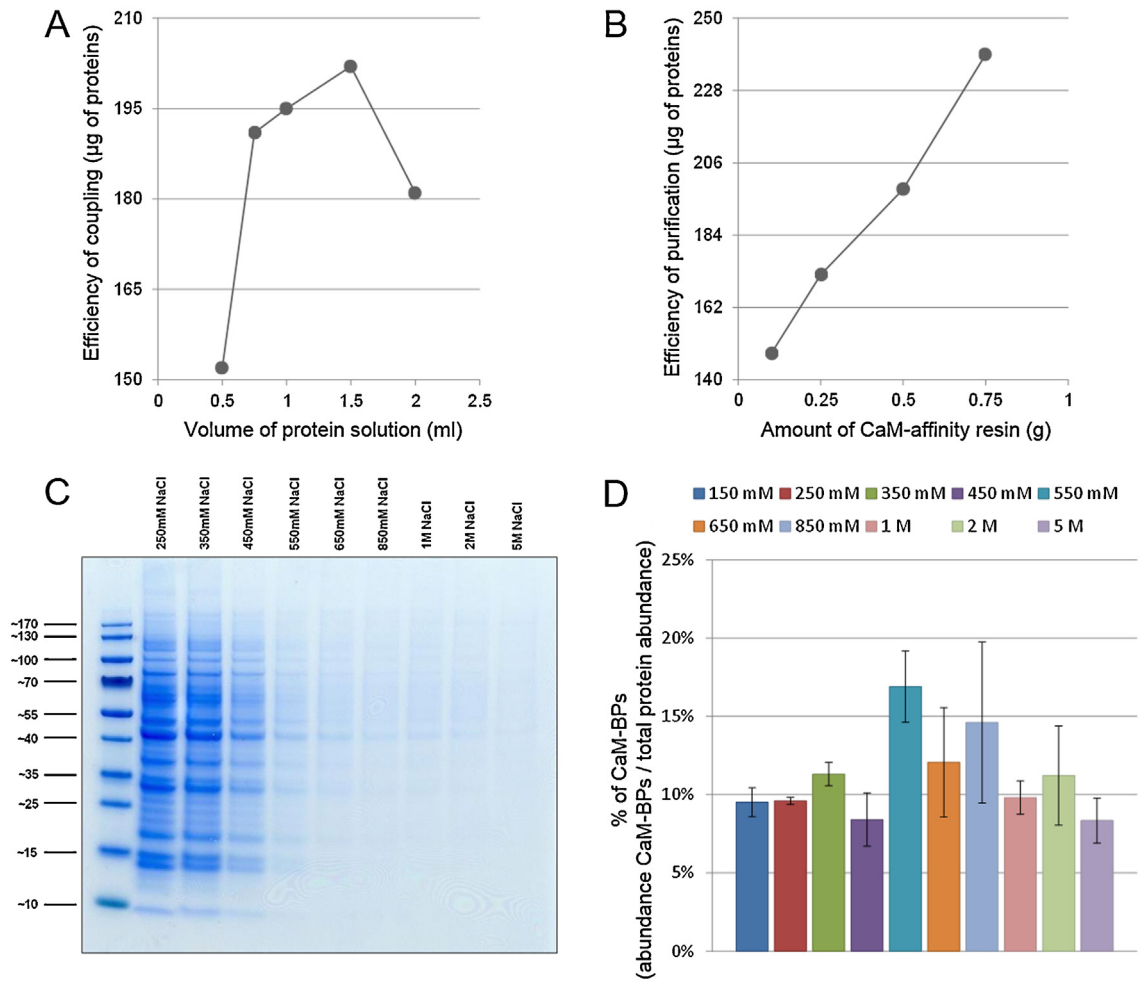

Fig. 2. Optimization of CaM-binding affinity purification. (A) Amount of proteins achieved from purification in relation to the volume of sample solution. Proteins captured on the beads were eluted by trypsin digestion on the resin. Efficiency of binding of CaM-BPs in each condition was assessed by amino acid analysis (AAA). To determine the real concentration of potential CaM-BPs from the eluted peptides using AAA, the amount of trypsin used for protein digestion was extracted from the final AAA results, and crude CaM-beads subjected to AAA were used as a control of the amount of CaM immobilized on the resin. (B) Amount of proteins achieved from purification in relation to amount of CaM-affinity resin. (C) SDS–PAGE analysis of protein content in each wash fraction (250 mM–5 M gradient of NaCl). Each NaCl wash was concentrated on ultrafiltration devices (3 kDa MW cut-off) to 50 μl and 90% of the sample volume was subsequently analyzed by SDS–PAGE. (D) The remaining 10% of each salt wash fraction was used to analyze percentage of CaM-BPs eluted by washing step at various salt concentrations. Data were analyzed by estimating the percentage of identified predicted CaM-BPs (only proteins with predicted CaM-binding motifs) compare to the total protein content in each wash fraction.

study of Ca^{2+}-dependent CaM-BPs requires presence of free Ca^{2+} and Mg^{2+} ions in the environment. Mg^{2+} ions are necessary for full activity of most of kinase enzymes. On the other hand, Ca^{2+} ions are required for activity of CaM-dependent kinases (e.g. CaMK kinase class of enzymes). Inability of using ion chelators (such as EDTA/EGTA), may be partially compensated by low temperature, which can significantly slow down the enzyme reaction rate.

Supplementary material related to this article found, in the online version, at http://dx.doi.org/10.1016/j.euprot.2015.05.004.

Hydrophobic interactions are known to play a significant role in CaM binding and ionic interactions are more commonly involved in non-specific interactions to both CaM and the resin [7]. We decided to use high ionic strength buffers to reduce non-specific protein binding to the CaM-affinity resin. To define the optimal washing condition the columns were washed with increasing NaCl (from 150 mM to 5 M) and each eluate was analyzed by SDS–PAGE. As expected, protein abundance decreased with increasing salt concentration (Fig. 2C and Table S1C). Using LC–MS/MS and label-free quantitative analysis of predicted CaM-BPs we estimated the concentration of NaCl in the wash buffer required for optimal purification of CaM-BPs. The relative abundance of CaM-BPs peaked in the 550 mM wash fraction (Fig. 2D). In parallel, we compared the specificity of a pull down where a gradient of salt wash was performed (from 150 to 450 mM NaCl) to the same volume of washing buffer containing only 150 mM NaCl (resin equilibrium buffer; see materials and methods). Results showed a trend, even though not significant, of more specific recovery of CaM-BPs (Fig. S4A). More in details, we verified that not using a gradient wash we recovered higher amount of common contaminants (Fig. S4B). Therefore, 450 mM NaCl was used as the final washing buffer in subsequent experiments.

Supplementary material related to this article found, in the online version, at http://dx.doi.org/10.1016/j.euprot.2015.05.004.

3.4. Protein-elution from the CaM-affinity resin

Using the conditions defined above to obtain optimal protein binding to the resin, we next focused on optimizing elution of the potential CaM-BPs. To release proteins bound to the resin, EGTA was first used to obtain the Ca^{2+}-dependent interactors. Then this was followed by surfactants (SDS) and organic solvents (MeOH) to obtain the Ca^{2+}-independent interactors. In the first step 10 mM EGTA was used in the elution buffer and 74 μg proteins was obtained from 0.5 mg mouse brain cytosol lysate using 0.5 ml of CaM-affinity resin (Table 2). After tryptic digestion and LC–MS/MS 271 potential CaM-BPs were identified of which 69 contained predicted CaM-binding motifs (Table S1D). Secondly, SDS plus MeOH was used to elute the Ca^{2+}-independent interactors since they strongly affect protein folding to potentially facilitate elution. AAA revealed the recovery of 114 μg of proteins from 0.5 mg mouse brain cytosol lysate. The samples were concentrated by $CHCl_3$–MeOH precipitation reducing protein recovery to 92 μg (Table 2). A total of 1068 potential CaM-BPs (186 proteins with CaM-binding motifs) were identified in this fraction (Table S1E). However, 211 of those proteins overlapped with the CaM-BP list obtained after EGTA elution. This suggests that 10 mM EGTA might not be sufficient to release all Ca^{2+}-dependent CaM-BPs from immobilized CaM, and a two-step elution (EGTA following SDS–MeOH) does not allow for separation of Ca^{2+}-dependent CaM-BPs from Ca^{2+}-independent ones.

Taking into consideration the above mentioned issue, a potentially simpler and more efficient elution approach is on-CaM-resin tryptic digestion. Optimal digestion of the total pool of CaM-BPs (instead of using EGTA and SDS-MeOH elutions) was performed in the presence of 20% ACN and peptides were eluted from the CaM-resin by centrifugation. The efficiency of each elution approach was also evaluated by boiling the beads after the elution step in SDS sample buffer prior to SDS–PAGE. Only the on-CaM-resin tryptic digestion allowed for complete protein elution from the CaM-affinity resin (Fig. S4C). Using AAA (and taking into account the amount of CaM protein on the resin) 226 μg of proteins were obtained using the tryptic digestion approach from 0.5 mg mouse brain cytosol lysate, about twice the amount compared with the above methods (Table 2). In this tryptic digest fraction 1732 putative CaM-BPs were identified (309 proteins with CaM-binding motifs) (Table S1F), up to 1.5 times more than the EGTA and SDS-MeOH elution's together. Overall the data suggests that many CaM-BPs are associated so strongly with CaM that they cannot be efficiently separated into Ca^{2+}-dependent and -independent interaction pools by the two-step elution strategy above.

3.5. Increasing the coverage of CaM-BPs with HILIC chromatography

To potentially increase protein coverage from the single-step CaM-affinity enrichment, especially of low abundance CaM-BPs, we performed sample fractionation. In order to decide which sample preparation provides a more in-depth quantification of our sample and its respective background control we compared SDS–PAGE and HILIC (Hydrophilic-Interaction Liquid Chromatography), two widely adopted fractionation strategies. Most previous CaM-affinity studies have used SDS–PAGE approaches [21–24]. However, SDS–PAGE is performed at the protein level; thus, we could not elute CaM-BPs from resin using on-column digestion. On the other hand, HILIC is performed at the peptide level, and it has been recently shown to increase coverage and sensitivity of LC–MS/MS analysis [33]. In these experiments we compared GeLC–MS/MS and HILIC on mouse brain CaM-affinity chromatography in the presence of Ca^{2+} ions. For GeLC–MS/MS, SDS-eluted proteins resolved on gels were excised as 13 gel bands and each subjected to in-gel trypsin digestion. Binding of background proteins to the beads was assessed in parallel using blank resin. We observed a 43% overlap between proteins identified in the CaM-BP pull down and the background (Table S2E). Missing values hindered confident quantitation of relative abundance between the two resins for many proteins, potentially due to non-uniform peptide losses during in-gel digestion and incomplete peptide extraction [48]. Non-uniform peptide losses ranging from 15 to 50% have been reported [49]. The total number of putative CaM-BPs identified

Table 2
Evaluation of various elution conditions of captured potential CaM-BPs from CaM affinity resin.

No.	10 mM EGTA (μg)	5% SDS/40% MeOH		On-column trypsin digestion (μg)[a]
		Before $CHCl_3$–MeOH precipitation (μg)	After $CHCl_3$–MeOH precipitation (μg)	
Rep. 1	70	116	96	183
Rep. 2	72	115	88	224
Rep. 3	80	112	92	272
Average	74	114	92	226

[a] Trypsin digestion on the resin: control sample with crude CaM-Sepharose resin was digested with trypsin in order to evaluate the concentration of CaM protein on the resin.

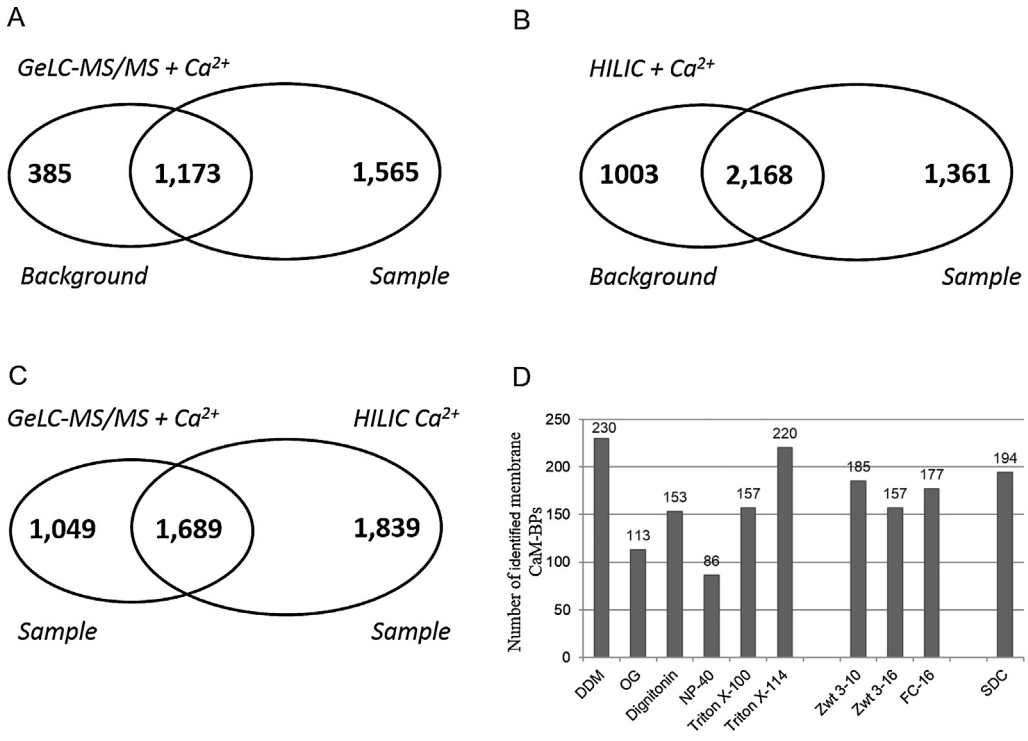

Fig. 3. Optimization of sample fractionation and purification of membrane CaM-BPs. Number of proteins identified in the sample (CaM-affinity resin) and background control (CNBr-Sepharose 4B resin) by using fractionation strategies such as SDS–PAGE (A) and HILIC (B). (C) Comparison of GeLC–MS/MS and HILIC LC–MS/MS strategies for the identification of putative CaM-BPs. (D) Analysis of detergent efficiency in purifying membrane associated predicted CaM-BPs. Detergents are non-ionic (left cluster), zwittergents (middle) and ionic (right cluster, only SDC). Membrane localization for the identified proteins is predicted by the presence of transmembrane domain (TM) and peripheral membrane (PM) proteins.

from the 13 gel bands fractions was 2738, of which 445 contained CaM binding motifs and 1173 overlapped with the background binding proteins (blank resin) (Fig. 3A and Table S2E).

Supplementary material related to this article found, in the online version, at http://dx.doi.org/10.1016/j.euprot.2015.05.004.

For the HILIC strategy, proteins bound to CaM-affinity or blank resin in the presence of Ca^{2+} were subjected to on-CaM-affinity resin trypsin digestion and the resulting peptides were separated by micro-HILIC HPLC fractionation prior to LC–MS/MS. A total of 16 peptide fractions were collected from the HILIC fractionation and the total number of identified proteins was 3529, of which 666 contained CaM binding motifs (Fig. 3B and Table S2A). In the blank sample 3171 proteins were identified of which 2168 overlapped those captured on CaM-affinity resin. A higher overlap (~61%) between sample and background was achieved, allowing a more confident discrimination between potential CaM-BPs and background binders. A comparison of the proteins detected in the two methods is shown in Fig. 3C. There was an overlap of 1689 proteins, but 790 more were detected only using the HILIC method. Overall, on-CaM-affinity resin digestion of bound proteins followed by HILIC remarkably increased the identification of putative CaM-BPs. Furthermore, HILIC allowed for better cross-sample quantitation due to better overlap of quantified proteins between sample and background control. The difference in abundance between sample and background control assisted removal of false positives from our CaM-BP list (Table S2A–E).

3.6. Pull down of membrane associated CaM-BPs

To enrich for the membrane associated CaM-BPs we investigated the performance of various detergents. Detergents were selected which cover a wide range of critical micelle concentration values and which belong to the group of ionic (bile salts) – e.g., sodium deoxycholate (SDC); non-ionic – e.g., *n*-dodecyl-β-D-maltoside (DDM), *n*-octyl-β-D-glucopyranoside (β-OG), Triton X-100, Triton X-114, NP-40, digitonin; and zwitterionc detergents – e.g., zwittergent 3–10, zwittergent 3–16 and FOS-CHOLINE-16 (FC-16) (Table 1; lists the detergents used). The tested detergents were used to solubilize the membrane pellet obtained from ultracentrifugation of total mouse brain lysate. CaM affinity chromatography for each detergent was performed in the presence of Ca^{2+} ions. Bound proteins were eluted and digested prior to LC–MS/MS using '*Method 2*' (Section 2.4). The overall strategy is summarized in Fig. S1.

We investigated the solubilization efficiency of membrane proteins in different protocols by observing the number of identified peripheral membrane (PM) and transmembrane (TM) proteins containing predicted CaM-binding motifs (predicted CaM-BPs) (Fig. 3D). The detergents were classified into three groups: Group 1 (the non-ionic detergents NP-40 and β-OG) contained detergents resulting in a low number of identified potential CaMBPs (≤113 proteins). Group 2 (the zwitterionic detergents FC-16, zwittergent 3–16 and zwittergent 3–10, as well as the non-ionic-detergent Digiton) allowed for identification of 1.5 fold more PM/TM CaMBPs (153–185 proteins). Group 3 (the non-ionic detergents Triton X-114 and DMM, as well as the ionic detergent SDC) detergents resulted in the highest number of purified PM/TM CaM-BPs (194–230 proteins). The classification of all identified PM and TM proteins in this study are shown in Table S1G.

The tested non-ionic group detergents allowed for the solubilization and affinity purification of 362 predicted membrane CaM-BPs. Those proteins covered various membrane associated cellular compartments without any particular organelle specificity. Ionic and zwitterionic detergents increased the number of identified membrane CaM-BPs by 68 proteins, which generally

represented the components of intra-cellular membranes such as mitochondrial, nucleus, and synaptic vesicle membranes (Fig. S6). This is consistent with the known ability of detergents with ionic and zwitterionic properties to be more suitable for solubilizing internal organelle membranes. Most nonionic detergents are relatively more effective in isolation of cytoplasmic proteins, while preserving internal organelle membranes. DDM was used in the subsequent studies.

Supplementary material related to this article found, in the online version, at http://dx.doi.org/10.1016/j.euprot.2015.05.004.

3.7. The CaM interactome from mouse brain

Next we applied the optimized method to identify the total amount of potential CaM-BPs from cytosolic and membrane fractions from mouse brains. Label-free quantitation was used to characterize genuine interacting proteins versus non-specific binders to the resin (Fig. S5). The list of identified putative CaM-BPs included only proteins significantly more abundant in the CaM-affinity pull-down in comparison with the blank binding control. The optimized on-CaM-affinity resin tryptic digestion workflow and HILIC fractionation revealed a total of 1900 cytosol and 1629 membrane proteins from both Ca^{2+}-dependent ($+Ca^{2+}$) and Ca^{2+}-independent ($\div Ca^{2+}$) condition (Fig. 5 and Table S3). Membrane proteins were defined by presence of TM or PM domains in their sequence. These 3529 proteins were next investigated for the presence of CaM binding motifs. A total of 696 proteins had predicted CaM binding motifs according to the Calmodulin Target Database [39]. Authentic CaM-BPs were validated using public databases and 170 proteins were found that were previously shown to have a CaM interaction. A total of 2663 novel putative CaM-BPs identified with our approach did not contain any known CaM binding consensus motif and were not previously described in the literature as CaM interactors. Since it is not yet possible to determine which of the specific binders are direct vs. indirect CaM-BPs, some of them might be secondary interactors. We also compared our data with a previously published list of CaM-BPs identified from mouse brain tissue using a high throughput method. Using CaM-affinity resin combined with GeLC–MS/MS, Berggård et al. and O'Connell et al. identified 140 putative CaM-BPs of which 87 contained predicted CaM binding motifs [21,50]. Our optimized protocol allowed near full coverage of this list, except for 8 proteins.

Supplementary material related to this article found, in the online version, at http://dx.doi.org/10.1016/j.euprot.2015.05.004.

All identified potential and known CaM-BPs were searched against the Gene Ontology (GO) database (http://www.geneontology.org) [51] included in GOrilla [38] and were grouped into

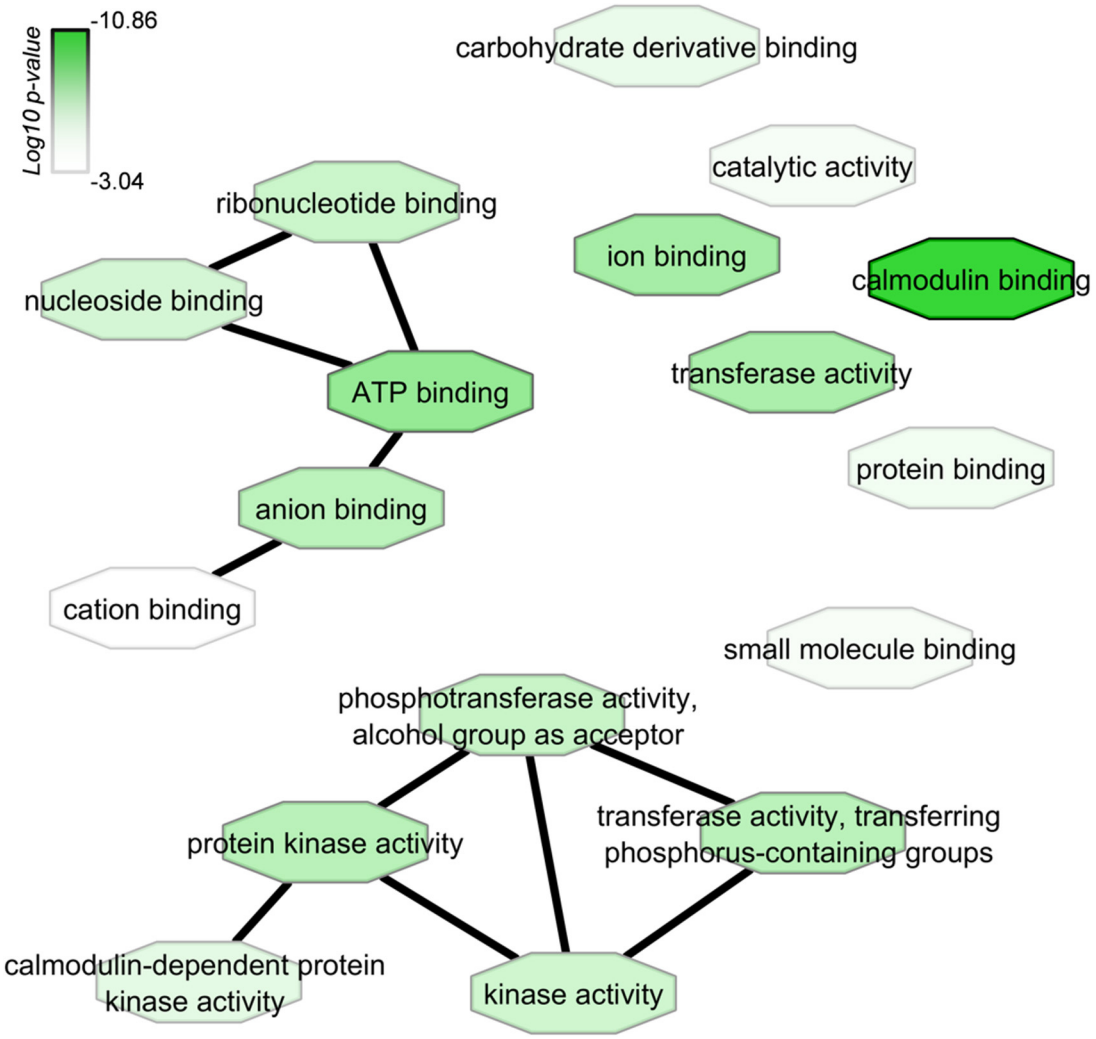

Fig. 4. Functional categories of identified CaM-BPs from the mouse brain tissue. Functional association analysis using the Gene Ontology Consortium (http://www.geneontology.org) included in GOrilla software was performed to determine if CaM-BPs were enriched in this study. Using a *P*-value color scale we indeed observed that a significant number of proteins were associated with CaM protein binding. In addition, many of the proteins identified were linked to biological processes regulated by CaM.

categories that define their biological process (Fig. 4). The highest GO enrichment was obtained for CaM binding function. Other highlighted groups included ATP-binding, ion-binding, and protein serine/threonine kinase activity such as CaM-dependent kinase activity. It has been reported that CaM regulates Ca^{2+}-dependent ATP hydrolysis and ATP-dependent Ca^{2+} transport in synaptic membranes [52]. For instance, Ohyama and coworkers have shown regulation of exocytosis through Ca^{2+}/ATP-dependent binding of autophosphorylated Ca^{2+}/CaM-activated protein kinase II to syntaxin 1A [53]. Synatxin 1A/HPC-1 is a key component of the exocytotic molecular machinery, namely, the soluble *N*-ethyl-maleimide-sensitive factor attachment protein (SNAP) receptor complex. Another example of the role of CaM in ATP-binding processes is described by Iwamoto et al., [54]. They showed that CaM interacts with the ATP binding cassette transporter A1 (ABCA1) to protect it from calpain-mediated degradation and up-regulates high-density lipoprotein generation. ABCA1 contains a typical CaM binding sequence of 1-5-8-14 motif (amino acid 1245–1257). The peptide covering this region showed binding to CaM, and deletion of the 1-5-8-14 motif abolished this interaction. Within the group of proteins showing kinase activity we identified a number of kinases which bind to CaM in the presence of Ca^{2+} ions, i.e. they are likely to be secondary interactors. The majority of proteins in this category were assigned to Ca^{2+}/CaM-dependent kinases like: Ca^{2+}/CaM -dependent protein kinase kinase I and II; Ca^{2+}/CaM-dependent protein kinase II subunit α and β; Ca^{2+}/CaM-dependent protein kinase type IV; Ca^{2+}/CaM-dependent protein kinase type I, IB, ID and IG. Noteworthy, we found 25 phosphatases or their regulatory subunits which are members of the PPP family protein serine/threonine phosphatases, which includes, PP1, PP2A, PP4, PP6, PP2B/calcineurin, PP2C, PP5 and PP7. PP1, PP2A, and PP2B, account for the majority of serine/threonine phosphatase activity in brain tissue [55]. PP1 and PP2A catalytic subunits are constitutively active, whereas PP2B is activated by binding of Ca^{2+}/CaM [56]. Within identified serine/threonine phosphatases only PP2B was previously described as a Ca^{2+}/CaM binding protein [57]. Interestingly, Quadroni et al., shown that CaM might serve as a substrate for some of the members of PPP family protein serine/threonine phosphatases, such as PP1γ and PP2A [58].

Next we classified the identified putative and known CaM-BPs from our data according to their subcellular localization and biological process which were retrieved from the Gene Ontology (GO) database (Fig. S7). A total of 652 proteins were annotated as originating from the cytoskeleton, 704 from plasma membrane and a range of proteins from other cell components (e.g., mitochondria (501 proteins), vacuole (86 proteins), endoplasmic reticulum (262 proteins), organelle lumen (654 proteins), extracellular space (222 proteins), Golgi apparatus (271 proteins), nucleus (1,430 proteins) and 26 proteins which are part of the secretory granule. Based on the annotation retrieved from the UniProt database (http://www.uniprot.org/), most of the identified CaM-BPs have multiple locations, while the detailed defined subcellular location could not be identified for 343CaM-BPs. A further in-depth classification with cellular function of the assigned CaM-BPs was conducted for the nuclear proteins as they were unexpectedly identified as a larger cellular compartment class. The proposed functions of nuclear CaM-BPs include protein binding as the largest group (984 proteins), followed by catalytic activity, metal ion binding, DNA binding, nucleotide and RNA binding (Fig. 7). In contrast, proteins that participate in e.g., transporter and translation regulator activity as well as receptor activity or signal transducer activity were present in smaller proportions (11–75 proteins). These results might support the idea that CaM plays a role in gene and protein expression [59,60]. The high number of identified nuclear, mitochondrial and other organelle lumen CaMBPs suggests that present methodology may also be applied in the study of organelle-specific CaMBPs.

Supplementary material related to this article found, in the online version, at http://dx.doi.org/10.1016/j.euprot.2015.05.004.

3.8. The Ca^{2+}-independent CaM interactome from mouse brain

Although much of the research has been focused around the roles of Ca^{2+}-CaM, the roles of apo-CaM are equally important but less clearly defined. In our study we also aimed to investigate CaM-BPs of the Ca^{2+}-independent type (÷Ca^{2+}). For this purpose, EGTA was present in the tissue lysates during the affinity enrichment step, to avoid interference from Ca^{2+}-dependent interactors.

From the total list described in the previous section (3529 CaM-BPs) we identified about five times less putative Ca^{2+}-independent cytosol CaM-BPs (261 proteins) compared to the Ca^{2+}-dependent analysis (1396 proteins) (Fig. 5). Interestingly, the overlap between the Ca^{2+}-dependent and -independent putative CaM-BPs was very high (243 proteins). A similar ratio was obtained from the membrane proteins (Fig. 5). This might be explained for some of the potential CaM-BPs since binding to CaM may be Ca^{2+}-dependent or Ca^{2+}-independent for different adjacent sites within the same protein, as observed for example in cytoplasmic unconventional myosin-I protein family (Myo). Myo proteins have two adjacent IQ-like motifs that each binds CaM but reveal opposite Ca^{2+} dependency. The N-terminal IQ motif binds CaM in the absence of Ca^{2+}, whereas the C-terminal IQ motif binds CaM in the presence of Ca^{2+} [61]. The Ca^{2+} sensitivity of proteins containing IQ motifs is highly variable and it has been shown that they can also bind to CaM in a Ca^{2+}-dependent manner. The

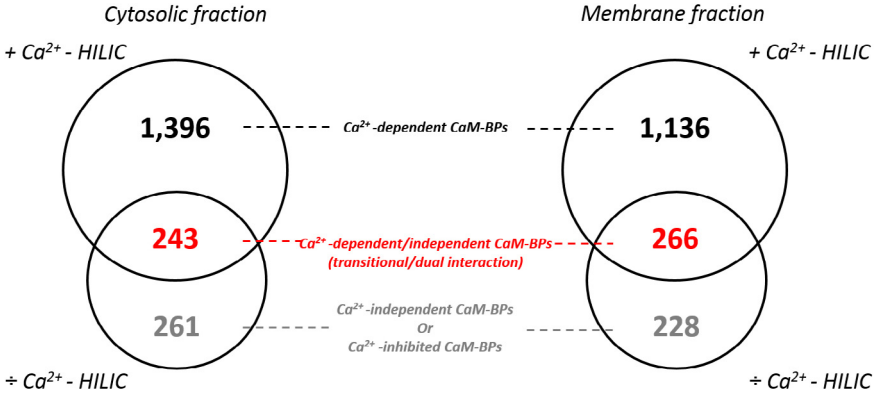

Fig. 5. Identification of CaM-BPs from mouse brain tissue. Different classes of CaM-BPs, highlighted their CaM binding dependence from Ca^{2+} ions, identified in the cytosolic and membrane fraction of mouse brain tissue. The numbers reflect the identification obtained by LC–MS/MS analysis preceded by HILIC fractionation.

transformation from Ca^{2+}-independent to Ca^{2+}-dependent binding appears to be due to a subtle amino acid substitution in the IQ recognition motif [62]. Proteins showing dual Ca^{2+}-dependency by IQ motifs also belong to the group of various receptors, ion exchangers, transporters, channels, IQ-motif-containing GTPase-activating proteins (IQGAP) e.g., ryanodine receptors, sodium/potassium-transporting ATPases, plasma membrane Ca^{2+} transporting ATPases, V-type proton ATPases, voltage-dependent Ca^{2+} channels, voltage-gated sodium channels, ras GTPase-activating-like proteins (IQGAP1-2). In many proteins the IQ motif may function in conjugation with a Ca^{2+}-dependent motif. Within the Ca^{2+}-dependent/-independent (transitional/dual) CaM-BPs we also identified many ribosomal proteins and other proteins associated with ribosomes (31 proteins) like e.g., elongation factor 2, 40S ribosomal protein S3a, 60S acidic ribosomal protein P1, 60S ribosomal protein L13, L19, L22 and L31, which have previously been reported to interact with CaM [63–65]. This was unexpected, as Behnen et al. showed that CaM binds to ribosome proteins in the presence of Ca^{2+} ions and thus plays an important role only in the Ca^{2+}-dependent regulation of protein synthesis [63].

CaM is phosphorylated by multiple protein-serine/threonine and protein-tyrosine kinases [66]. Casein kinase 2, myosin light chain kinase, tyrosine-protein kinase JAK1, proto-oncogene tyrosine-protein kinase Src and epidermal growth factor receptor are the well-established protein kinases implicated in this process. Interestingly, in our study all these proteins were identified as Ca^{2+}-independent CaM-BPs (bound only to apoCaM) with the exception of tyrosine-protein kinase JAK1, which was detected in the presence of Ca^{2+} ions. This indicates that the Ca^{2+}-loaded/CaM and the apo-CaM might be phosphorylated on different amino acid residues. Furthermore, we identified 37 other protein kinases and 8 phosphatases which might be regulated by Ca^{2+}-independent CaM interactions (e.g., casein kinase I isoform α and γ-1, tyrosine-protein kinase CSK, serine/threonine-protein kinase MRCK beta, serine/threonine-protein kinase MARK2, Ca^{2+}/CaM-dependent protein kinase kinase 1 and 2, receptor-type tyrosine-protein phosphatase γ). Most of these proteins do not contain IQ-motifs or other known consensus motifs for Ca^{2+}-independent CaM binding. This could support the hypothesis that some of the proteins regulated by apo-CaM are characterized by an unknown CaM binding mechanism [67].

3.9. Organelle-specific CaM interactome

Mammalian proteins are normally expressed in a variety of compartmentalized subcellular organelles and in specific cell types. Thus, characterization of organelle-specific CaM binding proteomes would contribute to better understanding the major signal-transduction pathways mediated by Ca^{2+}/CaM in these compartments. For example, a neuronal sub-structure such as the nerve terminals (synaptosomes), which represent less than 1% of the neuronal volume, are difficult to analyze from within a total brain homogenate. The selective isolation of synaptosomes is expected to reduce the dynamic range and aid in identification of synaptosome-enriched CaM-BPs. In particular, the primary function of synaptosomes is very dependent upon fast Ca^{2+} signaling. We therefore applied our optimized CaM-affinity enrichment method to purify CaM-BPs from synaptosomes isolated by percoll gradient centrifugation from rat brains.

In synaptosomes we identified a total of 2698 putative CaM-BPs, of which 168 were previously described in the literature and 439 contain predicted CaM binding motifs, supporting that they could be *bona fide* CaM-BPs (Fig. 6 and Table S4A). A total of 1348 cytosolic CaM-BPs and 1350 membrane CaM-BPs were identified. About half of the total of these two lists (1411 proteins) overlapped with the complete list of CaM-BPs identified above from the total mouse brain. They were primarily classified as constituents of functional categories such as CaM binding, Ca^{2+}-dependent protein binding, motor activity, structural constituent of ribosome, GTPase regulator activity, protein kinase activity, glutamate receptor activity, or structural molecule activity. Proteins which belong to these groups are generally present in high abundance in synaptosomes, thus they might be easily purified from total brain tissue homogenate. As expected, the synaptosome-enriched protein population (1287 proteins) primarily belonged to intra-synaptosomal compartments such as mitochondria, endosomes and synaptic vesicles, which are organelles-within-an-organelle (Fig. 6 and Table S4A). Several extracellular and integral to

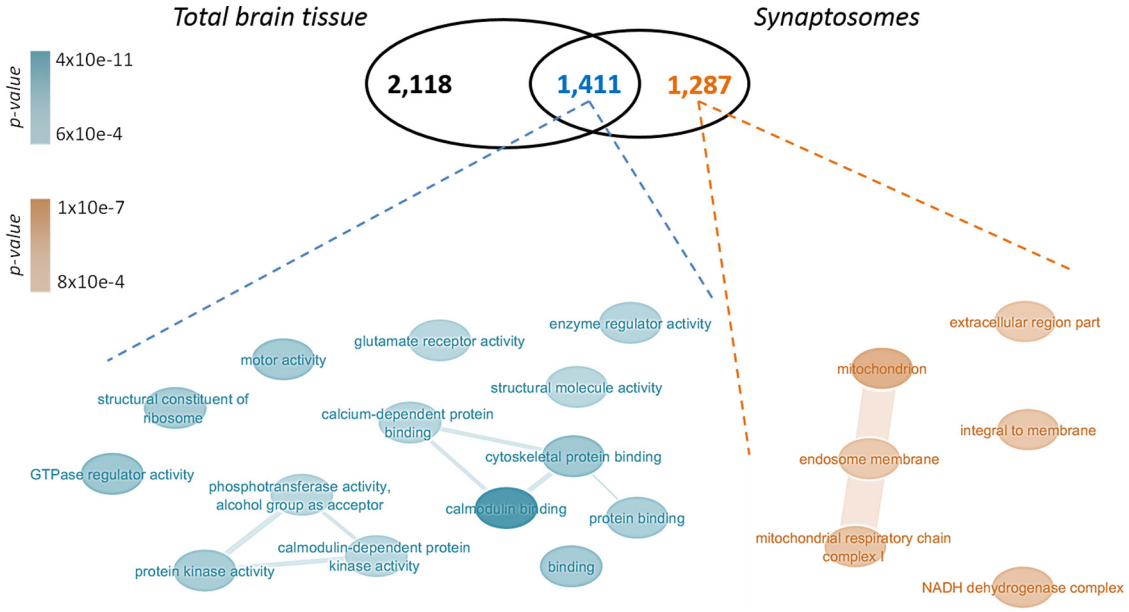

Fig. 6. Comparison of identified brain CaM-BPs with purified synaptosomal CaM-BPs. The organelle specific analysis of CaM-target interactions allowed for higher enrichment of CaM-BPs present in intra-synaptosomes compartments. The overlap between CaM-BPs from total brain tissue and synaptosomes concerned functional categories which have been characterized by proteins highly abundant in the cell and highly involved in CaM signaling.

peripheral membrane proteins were also identified as unique for the synaptosomal fraction. Many of those proteins are localized to the synaptic vesicles during synaptic vesicle recycling and this is consistent with the enrichment of synapses and active zones within the synaptosomes [68]. Current information describes four different pathways of synaptic vesicle protein internalization from the plasma membrane [69]. Some of those pathways involved passage of synaptic vesicles through an endosomal intermediate. The concentration of synaptic vesicles and endosomes is extraordinarily high in synaptosomes. This may explain the large number of identified extracellular and peripheral membrane proteins within the potential synaptosome CaM-BPs. Furthermore, the very high number of purified putative CaM-BPs in synaptosomes in comparison to the protein list obtained from total brain tissue highlights the importance of CaM-BPs in synaptic signaling and neurotransmitter release.

Supplementary material related to this article found, in the online version, at http://dx.doi.org/10.1016/j.euprot.2015.05.004.

3.10. Organelle-specific CaM-BP phosphoproteome

Recent studies of PTMs of CaM and its target proteins have prompted investigations into the role and mechanism of regulation of CaM and its targets by secondary regulatory pathways. It was shown that phosphorylation of CaM influences binding to CaM-BPs and results in important physiological consequences [70]. On the other hand, phosphorylation of CaM-BPs can also affect their binding to CaM. For instance, Jang et al., showed that there might exist four different classes of calcium- and phosphorylation-dependent CaM complexes [23].

To test the efficiency of our method in detecting phosphorylation of CaM-BPs, we performed CaM-affinity purification in the presence of Ca^{2+} ions on proteins extracted from rat synaptosomes. After on-CaM-resin tryptic digestion, the peptides were subjected to TiO_2 affinity chromatography to enrich phosphorylation sites within CaM-BPs. Subsequently, the phosphopeptide sample was fractionated by HILIC and analyzed by LC–MS/MS. A total of 2783 unique phosphopeptides (on 984 phosphoproteins) were identified on putative CaM-BPs from synaptosomes (Table S4B). The phosphorylated proteins captured on CaM-resin functionally belonged to CaM binding proteins, cytoskeletal proteins, protein binding proteins, metal ion transmembrane transporters, cation channels, GTPase activators, protein kinase binding proteins, receptors etc. (Fig. 7). This included e.g., synapsin-1, syntaxin-binding protein 5, amphiphysin, microtubule-associated protein 1A, protein piccolo, bassoon, or MARCKS which share a common involvement in synaptic transmission, long-term potentiation, synaptic depression, transport of synaptic vesicles, or release of neurotransmitter. Furthermore, identified putative CaM-BPs involved in ion transport (e.g., Ca^{2+}-activated potassium channel, sodium channel protein type 2), microtubule dynamics (e.g., myosin-9, neuromodulin, ankyrin-2, drebrin-1), or CaM-BPs related to axonal structure and neuron growth (e.g., creatine kinases, neural cell adhesion molecules, unconventional myosins, kinesin-like proteins) were also found in this study. Most of these proteins are known CaM-BPs or contain predicted CaM binding motifs. This could indicate the importance role of PTMs, such as phosphorylation, in regulation of CaM-target protein interaction or downstream signaling pathways. Collectively, this dataset represents a comprehensive mapping of phosphosites that belong to both well-known and putative synaptosomal CaM-BPs (Table S4C).

4. Conclusion

We have optimized the affinity enrichment of CaM-BPs using commercial CaM chromatographic material and applied the optimized method to characterize the whole mouse brain and synaptosome CaM binding proteome to identify new potential

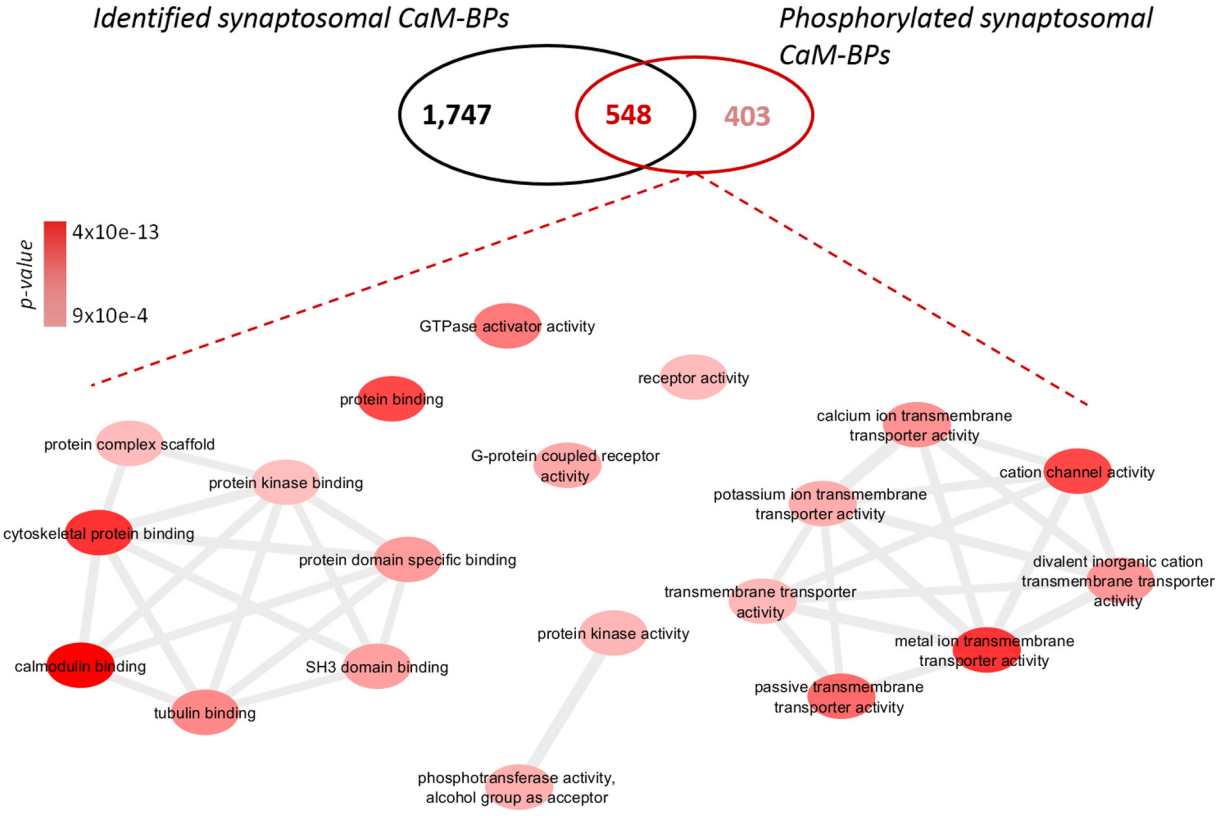

Fig. 7. Functional categories of identified putative phosphorylation-dependent CaM-BPs in the rat synaptosomes.

CaM-BPs. Sample pre-treatment with EGTA to remove Ca^{2+} ions from endogenous CaM-BP complexes prior to CaM affinity enrichment significantly increased the yield of potential CaM-BPs. The combination of affinity purification and MS with other techniques such as HILIC pre-fractionation and fractionation, quantitative proteomics or phosphopeptide enrichment significantly increases the number of confidently identified and characterized CaM-BPs. HILIC chromatography was used prior to LC–MS/MS to pre-fractionate tryptic peptides derived from direct proteolytic digestion of CaM-BPs on the CaM resin, resulting in nearly double amount of identified proteins compared to previous gel-based fractionation. Background binding control experiments were performed in parallel, using label free quantitation to exclude proteins binding to the CaM-affinity resin nonspecifically. Our optimized strategy allowed greatly improved detection of CaM-BPs in whole mouse brains and to identify the synaptosome CaM interactome for the first time.

In total we identified 3529 putative CaM-BPs from the brain and 2698 CaM-BPs from synaptosomes. We also identified 2783 unique phosphopeptides derived from potential synaptosomal CaM-BPs illustrating the potential for the method to identify the phosphoproteome of CaM interactomes. The CaM binding proteome analysis of total brain and isolated synaptosomes showed that CaM-BPs are unevenly distributed across cellular compartments and processes. This illustrates the heterogeneity in distribution of CaM target proteins and highlights the wide range of biological processes that are utilizing Ca^{2+}/CaM interaction in their regulation.

Taken together, this is to our knowledge the largest study of potential CaM-BPs in brain and synaptosomes, including the phosphorylation of synaptosomal CaM-BPs. Our optimized workflow can be further used to develop affinity capture strategies combined with LC-MS/MS to study protein–protein interactions and their dependency of PTMs. In addition, the lists of identified putative CaM-BPs, divided in Ca^{2+}-dependent or -independent, and cytosolic or membrane proteins obtained in this study have contributed significantly to the current knowledge about the growing CaM-binding interactome.

Conflict of interest

I hereby declare that there is no conflict of interest.

Acknowledgements

We are grateful for financial support from the Lundbeck Foundation (M.R.L. - Group Leader Fellowship) and the National Health & Medical Research Council Australia (P.J.R. Fellowship and Project grants), and for equipment from the Lundbeck Foundation (M.R.L. LTQ-Orbitrap Velos) the Australian Cancer Research Foundation, the Ramaciotti Foundation and the Cancer Institute NSW.

References

[1] C.B. Klee, T.C. Vanaman, Calmodulin, Adv. Protein Chem. 35 (1982) 213–321.
[2] D. Chin, A.R. Means, Calmodulin: a prototypical calcium sensor, Trends Cell Biol. 10 (8) (2000) 322–328.
[3] D.H. O'Day, CaMBOT: profiling and characterizing calmodulin-binding proteins, Cell Signal. 15 (4) (2003) 347–354.
[4] D.E. Clapham, Calcium signaling, Cell 131 (6) (2007) 1047–1058.
[5] M. Ikura, M. Osawa, J.B. Ames, The role of calcium-binding proteins in the control of transcription: structure to function, Bioessays 24 (7) (2002) 625–636.
[6] A.E. West, et al., Calcium regulation of neuronal gene expression, Proc. Natl. Acad. Sci. U. S. A. 98 (20) (2001) 11024–11031.
[7] A.P. Yamniuk, H.J. Vogel, Calmodulin's flexibility allows for promiscuity in its interactions with target proteins and peptides, Mol. Biotechnol. 27 (1) (2004) 33–57.
[8] S. Linse, A. Helmersson, S. Forsen, Calcium binding to calmodulin and its globular domains, J. Biol. Chem. 266 (13) (1991) 8050–8054.
[9] B.E. Finn, et al., Calcium-induced structural changes and domain autonomy in calmodulin, Nat. Struct. Biol. 2 (9) (1995) 777–783.
[10] S. Linse, T. Drakenberg, S. Forsen, Mastoparan binding induces a structural change affecting both the N-terminal and C-terminal domains of calmodulin. A 113Cd-NMR study, FEBS Lett. 199 (1) (1986) 28–32.
[11] M. Ikura, et al., Solution structure of a calmodulin-target peptide complex by multidimensional NMR, Science 256 (5057) (1992) 632–638.
[12] W.E. Meador, A.R. Means, F.A. Quiocho, Target enzyme recognition by calmodulin: 2.4 a structure of a calmodulin-peptide complex, Science 257 (5074) (1992) 1251–1255.
[13] C.F. Shuman, et al., Reconstitution of calmodulin from domains and subdomains: influence of target peptide, J. Mol. Biol. 358 (3) (2006) 870–881.
[14] P. James, T. Vorherr, E. Carafoli, Calmodulin-binding domains: just two faced or multi-faceted? Trends Biochem. Sci. 20 (1) (1995) 38–42.
[15] A. Crivici, M. Ikura, Molecular and structural basis of target recognition by calmodulin, Annu. Rev. Biophys. Biomol. Struct. 24 (1995) 85–116.
[16] A.R. Rhoads, F. Friedberg, Sequence motifs for calmodulin recognition, FASEB J. 11 (5) (1997) 331–340.
[17] M. Dasgupta, T. Honeycutt, D.K. Blumenthal, The gamma-subunit of skeletal muscle phosphorylase kinase contains two noncontiguous domains that act in concert to bind calmodulin, J. Biol. Chem. 264 (29) (1989) 17156–17163.
[18] M.R. Picciotto, A.J. Czernik, A.C. Nairn, Calcium/calmodulin-dependent protein kinase I. cDNA cloning and identification of autophosphorylation site, J. Biol. Chem. 268 (35) (1993) 26512–26521.
[19] J.S. Wolenski, Regulation of calmodulin-binding myosins, Trends Cell Biol. 5 (8) (1995) 310–316.
[20] M. Bahler, A. Rhoads, Calmodulin signaling via the IQ motif, FEBS Lett. 513 (1) (2002) 107–113.
[21] T. Berggard, et al., 140 mouse brain proteins identified by Ca2+-calmodulin affinity chromatography and tandem mass spectrometry, J. Proteome Res. 5 (3) (2006) 669–687.
[22] K.S. Kaleka, et al., Pull-down of calmodulin-binding proteins, J. Visualized Exp. (59) (2012) .
[23] D.J. Jang, M. Guo, D. Wang, Proteomic and biochemical studies of calcium- and phosphorylation-dependent calmodulin complexes in Mammalian cells, J. Proteome Res. 6 (9) (2007) 3718–3728.
[24] Z. Zhang, et al., Calmodulin-binding proteome in the brain, Methods Mol. Biol. 566 (2009) 181–190.
[25] P.R. Dunkley, P.E. Jarvie, P.J. Robinson, A rapid Percoll gradient procedure for preparation of synaptosomes, Nat. Protoc. 3 (11) (2008) 1718–1728.
[26] D. Wessel, U.I. Flugge, A method for the quantitative recovery of protein in dilute solution in the presence of detergents and lipids, Anal. Biochem. 138 (1) (1984) 141–143.
[27] M.J. Wall, et al., Implications of partial tryptic digestion in organic–aqueous solvent systems for bottom-up proteome analysis, Anal. Chim. Acta 703 (2) (2011) 194–203.
[28] C.G. Arsene, et al., Protein quantification by isotope dilution mass spectrometry of proteolytic fragments: cleavage rate and accuracy, Anal. Chem. 80 (11) (2008) 4154–4160.
[29] M.B. Strader, et al., Efficient and specific trypsin digestion of microgram to nanogram quantities of proteins in organic–aqueous solvent systems, Anal. Chem. 78 (1) (2006) 125–134.
[30] Y.L. Khmelnitsky, et al., Denaturation capacity – a new quantitative criterion for selection of organic–solvents as reaction media in biocatalysis, Eur. J. Biochem. 198 (1) (1991) 31–41.
[31] R. Batra, M.N. Gupta, Enhancement of enzyme-activity in aqueous–organic solvent mixtures, Biotechnol. Lett. 16 (10) (1994) 1059–1064.
[32] C. Polson, et al., Optimization of protein precipitation based upon effectiveness of protein removal and ionization effect in liquid chromatography-tandem mass spectrometry, J. Chromatogr. B Anal. Technol. Biomed. Life Sci. 785 (2) (2003) 263–275.
[33] K. Engholm-Keller, et al., TiSH–a robust and sensitive global phosphoproteomics strategy employing a combination of TiO2: SIMAC, and HILIC, J. Proteomics 75 (18) (2012) 5749–5761.
[34] A. Shevchenko, et al., Mass spectrometric sequencing of proteins silver-stained polyacrylamide gels, Anal. Chem. 68 (5) (1996) 850–858.
[35] G. Palmisano, et al., Selective enrichment of sialic acid-containing glycopeptides using titanium dioxide chromatography with analysis by HILIC and mass spectrometry, Nat. Protoc. 5 (12) (2010) 1974–1982.
[36] R. Apweiler, et al., Activities at the Universal Protein Resource (UniProt), Nucleic Acids Res. 42 (D1) (2014) D191–D198.
[37] E.et al. Eden, Discovering motifs in ranked lists of DNA sequences, PLoS Comput. Biol. 3 (3) (2007) e39.
[38] E. Eden, et al., GOrilla: a tool for discovery and visualization of enriched GO terms in ranked gene lists, BMC Bioinf. 10 (2009) 48.
[39] K.L. Yap, et al., Calmodulin target database, J. Struct. Funct. Genomics 1 (1) (2000) 8–14.
[40] H. Hermjakob, et al., IntAct: an open source molecular interaction database, Nucleic Acids Res. 32 (database issue) (2004) D452–5.
[41] B. Snel, et al., STRING: a web-server to retrieve and display the repeatedly occurring neighbourhood of a gene, Nucleic Acids Res. 28 (18) (2000) 3442–3444.
[42] G.D. Bader, et al., BIND–the biomolecular interaction network database, Nucleic Acids Res. 29 (1) (2001) 242–245.

[43] A. Zanzoni, et al., MINT: a molecular INTeraction database, FEBS Lett. 513 (1) (2002) 135–140.
[44] C. Stark, et al., BioGRID: a general repository for interaction datasets, Nucleic Acids Res. 34 (database issue) (2006) D535–D539.
[45] I. Xenarios, et al., DIP: the database of interacting proteins, Nucleic Acids Res. 28 (1) (2000) 289–291.
[46] A. Patil, K. Nakai, H. Nakamura, HitPredict: a database of quality assessed protein–protein interactions in nine species, Nucleic Acids Res. 39 (database issue) (2011) D744–D749.
[47] S. Peri, et al., Development of human protein reference database as an initial platform for approaching systems biology in humans, Genome Res. 13 (10) (2003) 2363–2371.
[48] B. Granvogl, P. Gruber, L.A. Eichacker, Standardisation of rapid in-gel digestion by mass spectrometry, Proteomics 7 (5) (2007) 642–654.
[49] T. Stewart II, Thomson, D. Figeys, 18O labeling: a tool for proteomics, Rapid Commun. Mass Spectrom. 15 (24) (2001) 2456–2465.
[50] D.J. O'Connell, et al., Integrated protein array screening and high throughput validation of 70 novel neural calmodulin-binding proteins, Mol. Cell Proteomics 9 (6) (2010) 1118–1132.
[51] M.A. Harris, et al., The Gene Ontology (GO) database and informatics resource, Nucleic Acids Res. 32 (database issue) (2004) D258–61.
[52] D.H. Ross, H.L. Cardenas, Calmodulin stimulation of Ca2+-dependent ATP hydrolysis and ATP-dependent Ca2+ transport in synaptic membranes, J. Neurochem. 41 (1) (1983) 161–171.
[53] A. Ohyama, et al., Regulation of exocytosis through Ca2+/ATP-dependent binding of autophosphorylated Ca2+/calmodulin-activated protein kinase II to syntaxin 1A, J. Neurosci. 22 (9) (2002) 3342–3351.
[54] N. Iwamoto, et al., Calmodulin interacts with ATP binding cassette transporter A1 to protect from calpain-mediated degradation and upregulates high-density lipoprotein generation, Arterioscler. Thromb. Vasc. Biol. 30 (7) (2010) 1446–1452.
[55] P.T. Cohen, Novel protein serine/threonine phosphatases: variety is the spice of life, Trends Biochem. Sci. 22 (7) (1997) 245–251.
[56] R.J. Colbran, Protein phosphatases and calcium/calmodulin-dependent protein kinase II-dependent synaptic plasticity, J. Neurosci. 24 (39) (2004) 8404–8409.
[57] T. Nakamura, et al., Ca2+/calmodulin-activated protein phosphatase (PP2B) of Saccharomyces cerevisiae. PP2B activity is not essential for growth, FEBS Lett. 309 (1) (1992) 103–106.
[58] M. Quadroni, et al., Phosphorylation of calmodulin alters its potency as an activator of target enzymes, Biochemistry 37 (18) (1998) 6523–6532.
[59] R.V. Kumar, et al., Inhibition of protein synthesis by antagonists of calmodulin in Ehrlich ascites tumor cells, Eur. J. Biochem. 195 (2) (1991) 313–319.
[60] H. Bito, K. Deisseroth, R.W. Tsien, Ca2+-dependent regulation in neuronal gene expression, Curr. Opin. Neurobiol. 7 (3) (1997) 419–429.
[61] M. Bahler, et al., Rat myr 4 defines a novel subclass of myosin I: identification, distribution, localization, and mapping of calmodulin-binding sites with differential calcium sensitivity, J. Cell Biol. 126 (2) (1994) 375–389.
[62] M. Bahler, A. Rhoads, Calmodulin signaling via the IQ motif, FEBS Lett. 513 (1) (2002) 107–113.
[63] P. Behnen, et al., Calcium-dependent interaction of calmodulin with human 80S ribosomes and polyribosomes, Biochemistry 51 (34) (2012) 6718–6727.
[64] G. Kaul, G. Pattan, T. Rafeequi, Eukaryotic elongation factor-2 (eEF2): its regulation and peptide chain elongation, Cell Biochem. Funct. 29 (3) (2011) 227–234.
[65] A.G. Ryazanov, Ca-2+ calmodulin-dependent phosphorylation of elongation factor-Ii, FEBS Lett. 214 (2) (1987) 331–334.
[66] G. Benaim, A. Villalobo, Phosphorylation of calmodulin – functional implications, Eur. J. Biochem. 269 (15) (2002) 3619–3631.
[67] L.A. Jurado, P.S. Chockalingam, H.W. Jarrett, Apocalmodulin, Physiol. Rev. 79 (3) (1999) 661–682.
[68] U. Distler, et al., In-depth protein profiling of the postsynaptic density from mouse hippocampus using data-independent acquisition proteomics, Proteomics 14 (21-22) (2014) 2607–2613.
[69] Y. Saheki, P. De Camilli, Synaptic vesicle endocytosis, Cold Spring Harbor Perspect. Biol. 4 (9) (2012) a005645.
[70] G. Benaim, A. Villalobo, Phosphorylation of calmodulin. Functional implications, Eur. J. Biochem. 269 (15) (2002) 3619–3631.